

Investigation of the Transcriptomic Response of Atlantic Salmon (*Salmo Salar*) Exposed to *Paramoeba Perurans* Using Next Generation Sequencing

Anita Talbot (✉ anita.talbot@gmit.ie)

Galway-Mayo Institute of Technology

Laura Gargan

University College Dublin

Grainne Moran

Galway-Mayo Institute of Technology

Louis Prudent

Galway-Mayo Institute of Technology

Ian O'Connor

Galway-Mayo Institute of Technology

Luca Mirimin

Galway-Mayo Institute of Technology

Jens Carlsson

University College Dublin

Eugene MacCarthy

Galway-Mayo Institute of Technology

Research Article

Keywords: Amoebic Gill Disease (AGD), *Paramoeba perurans*, Differentially Expressed Genes (DEGs), Reactome Gene Sets

Posted Date: January 22nd, 2021

DOI: <https://doi.org/10.21203/rs.3.rs-142213/v1>

License:  This work is licensed under a Creative Commons Attribution 4.0 International License.

[Read Full License](#)

Abstract

Amoebic Gill Disease (AGD), caused by the protozoan extracellular parasite *Paramoeba perurans*, is a disease affecting Atlantic salmon (*Salmo salar*) aquaculture. Many studies to date have investigated the pathogenesis of AGD focusing on the host immune response in the gill after the appearance of clinical symptoms. This study investigated the gill transcriptomic profile of pre-clinical AGD using RNA-sequencing (RNA-seq) technology. RNA-seq libraries generated at 4, 7, 14 and 16 days post inoculation (dpi) identified 29,357 Differentially Expressed Genes (DEGs). RNA-seq data was validated using real-time, quantitative PCR (qPCR) analysis of 10 selected immune genes. DEGs mapped to 224 Gene Ontology (GO) terms, 27 reference pathways in the Kyoto Encyclopedia of Genes and Genomes (KEGG) and 15 Reactome Gene Sets. Immune suppression was evident at 7 dpi, prior to there being any evidence of AGD on the gill, involving signalling pathways for interleukins, Nod-like receptors, B-cell and T-cell receptors, and the differentiation of Th1/Th2 and Th17 cells. The results of this study suggest a mechanism for how *N. perurans* circumvents the host immune response to establish a successful infection, and could potentially lead to the development of novel strategies for AGD mitigation or prevention in aquaculture.

Introduction

Amoebic Gill Disease (AGD) is a proliferative gill disease of marine cultured Atlantic salmon, with the aetiological agent being the free-living protozoan *Paramoeba perurans*¹. Among the parasitic conditions affecting gill health, AGD is the most significant in terms of prevalence and economic impact². First described in Tasmania in 1985¹, AGD is now present in all Atlantic salmon producing countries. Infection of the gill with *Paramoeba sp.* is reported to induce a tri-phasic host response, including a localised reaction to adhered parasites, a non-specific immuno-regulatory cell infiltration and advanced hyperplasia with epithelial stratification filaments³. Macroscopically, AGD lesions are visible as white raised mucoid patches on the gill, as a result of increased mucus production by mucous cells, which forms the basis of the gross gill score scheme developed by Taylor et al. (2009)⁴ to monitor the progress of AGD. In advance of gill pathology, the presence of *P. perurans* can be detected using a diagnostic real-time PCR (qPCR)⁵. The treatment for diagnosed AGD is either freshwater (< 3 PSU for 3 hours) or hydrogen peroxide (H₂O₂) (800–1300 ppm for < 20 minutes) baths⁶.

To date, investigations focusing on differential gene expression AGD in salmon have utilised techniques such as microarray analysis^{7–9}, Polymerase Chain Reaction (PCR)^{10–15}, ribonucleic acid sequencing (RNA-seq) and single nucleotide polymorphism (SNP) analysis¹⁶.

Previous AGD studies identified up-regulation of the pro-inflammatory cytokine, interleukin-1beta (IL-1b) as being the hallmark of advanced stage AGD in Atlantic salmon^{11,13}. A recent study using 2D quantitative RT-PCR found AGD-affected gills displayed an increased mRNA expression of cellular

markers of immune cells, including professional antigen presenting cells (MHC-II, CD4), B cells (IgM, IgT, MHC-II) and T cells (TCR, CD4, CD8) ¹⁴.

The down-regulation of tumour suppressor p53 (p53) has been suggested as one of the mechanisms underlying cell proliferation in AGD⁷. The differential expression of genes involved in oxidative stress has also been reported¹⁷.

Th1, Th17 and T-reg pathways were found to be down-regulated in AGD infections initiated with a higher dose of amoeba (5000 amoeba/L) with the Th2 pathway up-regulated by both high and low infection doses (500 and 5000 amoeba /L)¹⁰. Th2 cytokines, (il4/13a and il4/13b2), and the mucin Muc5AC have also been found to be up-regulated in the gill in AGD¹². The aim of the current study was to investigate the early-phase transcriptomic host response of naïve salmon inoculated with *P. perurans* using Next Generation Sequencing (NGS), specifically RNA-seq, prior to the onset of gill pathology. As RNA-seq can be used as a discovery-based technique, it does not require prior knowledge of the genomic information related to genes of interest, with the advantage of facilitating the identification of both known and unknown transcripts.

Results

Clinical symptoms of AGD were determined by macroscopic examination of the intact gills and were scored ranging from 0 (absence of clinical symptoms) to 5 (extensive lesions covering most of the gills surface) ⁴. No lesions were evident on the gills in AGD-infected groups at 4 and 7 dpi, with 3/6 fish at gill score 1 at 14 dpi, and 6/6 fish with gill score 1 at 16 dpi. Diagnostic qPCR⁵ analysis of the gill arch samples confirmed the presence of *P. perurans* in 5/6 at 4 dpi, 6/6 fish at 7 dpi and 14 dpi and in 5/6 fish at 16 dpi. There was no *P. perurans* detected in any of the control fish sampled at any time point. Gills were examined microscopically following staining with haematoxylin/eosin at all time points (Fig. 2). Evidence of hyperplasia and fusion of the lamellar epithelium (Fig. 2b) was observed at 16 dpi.

Mapping RNA-seq reads to reference genome

The analysis of the reads mapped to the *Salmo salar* reference genome for the 6 fish from each of the 5 sampling time points (0, 4, 7, 14 and 16 dpi) is presented in supplementary Table S1 online. The sequencing depth for each fish ranged from 21.7M to 35.4M raw reads. The % GC ranged from 47 to 49%. The % clean paired reads ranged from 88.4 to 94.7%. The number of assigned fragments or feature counts range was 14.7M to 25.1M.

Validation of RNA-seq data using qPCR

Ten immune genes from the gill RNA-seq data were selected for qPCR validation across all sampling time points including cathelicidin 1 (*cath-1*), c-type lectin receptor A (*clr-A*), c-c motif chemokine 4 (*cxc4*), immunoresponsive 1 homolog/aconitate decarboxylase 1 (*irg1/acod1*), interleukin-8 (*il-8*), interleukin-17F (*il-17*), leukocyte cell-derived chemotaxin-2, (*lect2*), inducible nitric oxide synthase 2, (*nos2*), serum

amyloid P (*sap*) and pentraxin-related protein (*ptx3*). Primer sequences are provided in supplementary Table S2 online. A Spearman correlation analysis of the RNA-seq and the qPCR data using the Log₂ fold change (FC) average of 6 individual fish per gene was conducted for all 4 time points: 4 dpi: s = 14.5, rho = 0.91, p < 0.0002, 7 dpi: s = 16.5, rho = 0.89, p < 0.0003, 14 dpi: s = 36.2, rho = 0.78, p < 0.008, 16 dpi: s = 14.1, rho = 0.91, p < 0.0002. The results of the 16 dpi RNA-seq and qPCR validation data are presented in Fig. 3a with the corresponding correlation data in Fig. 3b.

Differentially Expressed Genes (DEGs)

Differentially expressed genes were identified at each of the four experimental time points (4,7,14 and 16 dpi) (Fig. 1), and further divided into up-regulated and down-regulated genes for a total of 8 DEG lists.

A total of 29,357 genes were found to be differentially regulated in the gill as a result of AGD infection, with approximately equal numbers of up- and down-regulated genes (Table 1). The %DEGs at 4, 14 and 16 dpi ranged from 16.5–21.9% with a higher % of genes down-regulated genes than up-regulated (61.7%, 52.4% and 54.7%, respectively). At 7 dpi there were 42.3% DEGs, with more up-regulated than down-regulated (59.4% vs 40.4%).

Table 1
Differentially Expressed Genes (DEGs)

Time (dpi)	Up-regulated	Down-regulated	Up- and down-regulated	% of total
4	1,853 (38.3%)	2,985 (61.7%)	4,838	16.5
7	7,408 (59.6%)	5,024 (40.4%)	12,432	42.3
14	2,698 (47.6%)	2,971 (52.4%)	5,669	19.3
16	2,905 (45.3%)	3,513 (54.7%)	6,418	21.9
Total	14,864 (50.6%)	14,493 (49.4%)	29,357	100

Gene Ontology (GO) and Pathway Enrichment

At 4 dpi, the GO:0002768: immune response-regulating cell surface receptor signalling pathway (Fig. 4a) was identified as being enriched up-regulated DEGs with GO: 0042254: ribosome biosynthesis, the most significant term enriched with down-regulated DEGS at 4 dpi (Fig. 4b). No enriched pathways were identified with up-regulated DEGs, however 6 pathways were identified with down-regulated DEGs including dre03008: Ribosome biogenesis in eukaryotes being the most significant (Table 2).

At 7 dpi, fourteen enriched pathways were identified with dre04146: peroxisome being the most significant (Table 2). Seven pathways were identified with the dre04110: cell cycle pathway being the most significantly enriched (Table 2). Pathways relevant to AGD infection included dre04115: p53 signalling pathway and R-DRE-168256: immune system of which subsets included R-DRE-168249: innate immune system R-DRE-1280215: cytokine signalling in immune system and R-DRE-449147: signalling by interleukins (Table 2).

At 14 dpi, the reactome gene set R-DRE-983695: antigen activates b-cell receptor (BCR) leading to generation of second messengers pathway was the only enriched pathway (Table 2). At 14 dpi eight pathways were enriched with dre03030: DNA replication as the most significant (Table 2).

At 16 dpi, one KEGG pathway was found to be enriched, dre00380: Tryptophan metabolism with 4 reactome gene sets also identified including R-DRE-983695: Antigen activates B Cell Receptor (BCR) leading to generation of second messengers (Table 2). At 16 dpi for the down-regulated genes, fifteen pathways were identified (8 KEGG, and 7 reactome gene sets), with the most significant being dre03008: Ribosome biogenesis in eukaryotes (Table 2). Of immune relevance was R-DRE-983170: antigen presentation of class I MHC.

Table 2
Pathways enriched with Differentially Expressed Genes (DEGs).

Time / gene expression direction	Category	Term	Description	-10 Log(P)	InTerm / InList
4dpi/down	KEGG Pathway	dre03008	Ribosome biogenesis in eukaryotes	10.2	22/37
		dre03040	Spliceosome	7.1	23/53
		dre03050	Proteasome	6.9	13/20
		dre03030	DNA replication	6.6	15/27
		dre00100	Steroid biosynthesis	4.7	7/9
		dre04141	Protein processing in endoplasmic reticulum	4.6	20/57
7 dpi/up	KEGG Pathway	dre04146	Peroxisome	9.9	31/45
		dre01212	Fatty acid metabolism	8.4	20/25
		dre03010	Ribosome	7.5	28/45
		dre00071	Fatty acid degradation	7.4	17/21
		dre00380	Tryptophan metabolism	6.9	14/16
		dre00260	Glycine, serine and threonine metabolism	6.8	15/18
		dre04142	Lysosome	6.3	29/52
		dre00280	Valine, leucine and isoleucine degradation	6.0	18/26
		dre00340	Histidine metabolism	5.9	11/12
		dre03320	PPAR signaling pathway	4.9	17/27
		dre01040	Biosynthesis of unsaturated fatty acids	4.8	9/10
		dre00410	beta-Alanine metabolism	4.7	12/16
		dre00310	Lysine degradation	2.9	13/24
		dre00640	Propanoate metabolism	2.1	9/17
7 dpi/down	KEGG Pathway	dre04110	Cell cycle	7.1	20/138
		dre03030	DNA replication	5.3	9/38
		dre00520	Amino sugar and nucleotide sugar metabolism	3.8	9/57

Time / gene expression direction	Category	Term	Description	-10 Log(P)	InTerm / InList
		dre04115	p53 signaling pathway	2.9	9/75
		dre00230	Purine metabolism	2.4	15/196
		dre00240	Pyrimidine metabolism	2.3	10/107
	Reactome Gene Sets	R-DRE-168256	Immune System	4.6	51/790
		R-DRE-168249	Innate Immune System	3.5	31/449
		R-DRE-449147	Signaling by Interleukins	2.2	14/185
		R-DRE-1280215	Cytokine Signaling in Immune system	-2.2	16/227
14 dpi/up	Reactome Gene Sets	R-DRE-983695	Antigen activates B Cell Receptor (BCR) leading to generation of second messengers	2.7	3/6
14 dpi/down	KEGG Pathway	dre03030	DNA replication	9.6	17/27
		dre03008	Ribosome biogenesis in eukaryotes	8.5	19/37
		dre03040	Spliceosome	4.2	17/53
		dre00240	Pyrimidine metabolism	3.9	15/46
		dre03050	Proteasome	3.0	8/20
		dre01212	Fatty acid metabolism	2.9	9/25
		dre00230	Purine metabolism	2.2	18/84
		dre00280	Valine, leucine and isoleucine degradation	2.1	8/26
16 dpi/up	KEGG Pathway	dre00380	Tryptophan metabolism	2.1	4/16
	Reactome Gene Sets	R-DRE-983695	Antigen activates B Cell Receptor (BCR) leading to generation of second messengers	2.6	3/6
		R-DRE-1433557	Signaling by SCF-KIT	2.6	3/6
		R-DRE-373752	Netrin-1 signaling	2.3	3/7
		R-DRE-9007101	Rab regulation of trafficking	2.1	5/24

Time / gene expression direction	Category	Term	Description	-10 Log(P)	InTerm / InList
16 dpi/down	KEGG Pathway	dre03008	Ribosome biogenesis in eukaryotes	9.5	22/37
		dre03030	DNA replication	5.2	14/27
		dre00240	Pyrimidine metabolism	4.4	18/46
		dre00100	Steroid biosynthesis	4.4	7/9
		dre00970	Aminoacyl-tRNA biosynthesis	3.9	12/26
		dre03050	Proteasome	3.7	10/20
		dre03013	RNA transport	3.6	20/61
		dre03040	Spliceosome	3.5	18/53
	Reactome Gene Sets	R-DRE-8953854	Metabolism of RNA	5.5	34/106
		R-DRE-1640170	Cell Cycle	3.7	32/116
		R-DRE-983170	Antigen Presentation of Class I MHC	2.5	3/3
		R-DRE-77286	Mitochondrial fatty acid beta-oxidation	2.5	3/3
		R-DRE-212300	PRC2 methylates histones and DNA	2.5	3/3
		R-DRE-2262752	Cellular responses to stress	2.4	15/50
R-DRE-8953897	Cellular responses to external stimuli	2	19/74		

At 4, 14 and 16 dpi process and pathway enrichment identified 14 up-regulated genes with involvement in immune regulation and activation (Table 3). Immune biological processes and a reactome gene set (Table 2) were identified from the DEG lists generated at each time point and are listed in Table 3 and included GO:0002682: Regulation of immune system process (btk, c1cq, CD79b, CD99, cgas, hmgb1a, hmgb3b, Il-34, kita, lyn, tfpi1, themis), GO:0002253: Activation of immune system process (btk, c1cq, CD79b, cgas, hmgb1a, themis), GO:0097190: B-cell differentiation (kita, cd79b and Ikzf1.7), GO:0002768: immune response-regulating cell surface receptor signalling pathway (kita, btk, cd79b, themis2). The reactome gene set is R-DRE-983695: Antigen activates B Cell Receptor (BCR) leading to generation of second messengers (dapp, btk, and CD79b).

Table 3
Up-regulated genes with involvement in immune regulation and activation

Gene ID	Gene	Name	Biological Process and Pathway	dpi
568653	btk	Bruton agammaglobulinemia tyrosine kinase	GO:0002682 GO:0002253 R-DRE-983695	14, 16
449803	c1qc	complement component 1, q subcomponent, C chain	GO:0002682 GO:0002253	14, 16
100329481	cd79b	CD79b molecule, immunoglobulin-associated beta	GO:0002682 GO:0002253 GO:0097190 GO:0002768 R-DRE-983695	4, 14, 16
559896	cd99	CD99 molecule	GO:0002682	14
557043	cgas	cyclic GMP-AMP synthase	GO:0002682 GO:0002253	14, 16
550386	dapp1	dual adaptor of phosphotyrosine and 3-phosphoinositides	R-DRE-983695	14, 16
321622	hmgb1a	high mobility group box 1a	GO:0002682 GO:0002253	14, 16
550466	hmgb3b	high mobility group box 3b	GO:0002682	14
560193	il34	interleukin 34	GO:0002682	14
30256	kita	KIT proto-oncogene, receptor tyrosine kinase a	GO:0002682 GO:0097190 GO:0002768	4, 14, 16
30177	ikzf1	IKAROS family zinc finger 1	GO:0097190	14, 16
447804	lyn	LYN proto-oncogene, Src family tyrosine kinase	GO:0002682	14
560339	tfpi2	tissue factor pathway inhibitor 2	GO:0002682	14
100535600	themis2	thymocyte selection associated family member 2	GO:0002682 GO:0002253 GO:0002768	4, 14, 16

At 7 dpi the reactome gene set R-DRE-168256: immune system (Table 2) was associated with 51 down-regulated genes (Table 4). Within this reactome gene set, 16 genes were associated with R-DRE-1280215: cytokine signalling in the immune system with all but 2 of these genes associated with R-DRE-449147:

signalling by interleukins (Table 2). Screening of the DEG lists at 7 dpi identified multiple transcripts for 9 members of the interleukin family as being down-regulated (IL-1 β , IL-8, IL-11, IL-12 β , IL-15, IL-17D, IL-17F, IL-18, IL-34) with only one member, IL-27 β significantly up-regulated (12.4 log₂FC) (supplementary Table S3 online). Functional enrichment analysis (string-de.org) using the 51 genes identified in R-DRE-168256: immune system genes at 7 dpi (Table 4) identified involvement in the Nod-like receptor signalling pathway (hsa04621, FDR 8.58e-08: *cxcl8*, *hsp90AB1*, *ikbkb*, *irf9*, *mapk3*, *nlrx1*, *sugt1*, *tbk1*, *traf3*), B-cell receptor signalling (hsa-04662, FDR 0.0051: *ikbkb*, *mapk3*, *sky*), T-cell receptor signalling (hsa-04660, FDR 0.0106: *dlg1*, *ikbkb*, *mapk3*), Th1/Th2 cell differentiation (hsa-04658, FDR 0.00084: *ikbkb*, *jak3*, *mapk3*, *stat4*) and Th17 cell differentiation (hsa-04659, FDR 0.0011: *hsp90ab1*, *ikbkb*, *jak3*, *mapk3*).

The pattern and extent of DEGs at 7 dpi was different from the other time points with more genes showing differential expression (42%) and with more genes being up-regulated (59.6%) (Table 1).

Analysis of the DEG lists at 7 dpi found that of the top 100 up-regulated genes there were 87 characterised and 69 unique transcript (supplementary Table S4 online). The most up-regulated gene was mannan binding lectin serine peptidase 2 (*masp2*, 30.0 log₂FC). Thirteen other complement transcripts were also up-regulated including (C1q-like protein 2 (x4), C1q-like protein 3, C2-like, C3-like (x2), C9, factor B, factor H, properdin-like (x2). Acute Phase Response (APR) genes in the top 100 included pentraxin, alpha-1-antitrypsin (x2), alpha-2-macroglobulin (x2), fibrinogen (α , β , γ), leukocyte cell-derived chemotaxin-2 (*lect2*), serum amyloid P-component (SAP).

The top 100 down-regulated genes at 7 dpi yielded 78 unique transcripts and 19 uncharacterised genes (supplementary Table S5 online). The genes that were represented by multiple transcripts included C-C motif chemokine 4-like (2x), collagenase 3-like (2x), interferon-induced very large GTPase 1-like (2x), NADPH oxidase organizer 1-like (2x). The gene with the most down-regulated expression was interferon-induced guanylate-binding protein 1-like (log₂FC, -7.5). Multiple members of the same gene family included the c-c chemokine family (*cc4*, *cc20*), the interleukins (*il-1b*, *il-17F*, *il-17* receptor E), and mucins (*muc2*, *muc7*).

Table 4
Immune relevant down-regulated genes and associated reactome gene sets at 7 dpi

Gene ID	Gene	Name	Reactome Gene Sets
336425	aldoaa	aldolase a, fructose-bisphosphate, a	R-DRE-168256, R-DRE-168249
114428	arf1	ADP-ribosylation factor 1	R-DRE-168256
415204	arpc3	actin related protein 2/3 complex, subunit 3	R-DRE-168256, R-DRE-168249
767630	atp8a1	ATPase phospholipid transporting 8A1	R-DRE-168256, R-DRE-168249
192322	calm2b	calmodulin 2b, (phosphorylase kinase, delta)	R-DRE-168256, R-DRE-168249
334527	cap1	CAP, adenylate cyclase-associated protein 1	R-DRE-168256, R-DRE-168249
394037	cct8	chaperonin containing TCP1, subunit 8 (theta)	R-DRE-168256, R-DRE-168249
567192	cd59	CD59 molecule (CD59 blood group)	R-DRE-168256, R-DRE-168249
767754	cenpe	centromere protein E	R-DRE-168256
336381	cotl1	coactosin-like F-actin binding protein 1	R-DRE-168256, R-DRE-168249
100134935	csf3r	colony stimulating factor 3 receptor (granulocyte)	R-DRE-168256, R-DRE-1280215, R-DRE-449147
30265	ctnnb1	catenin (cadherin-associated protein), beta 1	R-DRE-168256
100002946	cxcl8a	chemokine (C-X-C motif) ligand 8a	R-DRE-168256
336613	cyfip1	cytoplasmic FMR1 interacting protein 1	R-DRE-168256, R-DRE-168249
324089	det1	DET1 partner of COP1	R-DRE-168256
114446	dlg1	discs, large homolog 1 (Drosophila)	R-DRE-168256, R-DRE-1280215, R-DRE-449147
100005297	epgn	epithelial mitogen homolog (mouse)	R-DRE-168256, R-DRE-1280215, R-DRE-449147
562999	hectd2	HECT domain containing	R-DRE-168256
30573	hsp90ab1	heat shock protein 90, alpha (cytosolic), class B member 1	R-DRE-168256, R-DRE-168249
563560	ikbkb	inhibitor of nuclear factor kappa B kinase subunit beta	R-DRE-168256, R-DRE-168249, R-DRE-1280215

Gene ID	Gene	Name	Reactome Gene Sets
560193	il34	interleukin 34	R-DRE-168256, R-DRE-1280215, R-DRE-449147
403013	irf9	interferon regulatory factor 9	R-DRE-168256, R-DRE-1280215, R-DRE-449147
561370	jak3	Janus kinase 3 (a protein tyrosine kinase, leukocyte)	R-DRE-168256, R-DRE-1280215, R-DRE-449147
555969	lpcat1	lysophosphatidylcholine acyltransferase 1	R-DRE-168256, R-DRE-168249
399480	mapk3	mitogen-activated protein kinase 3	R-DRE-168256, R-DRE-168249, R-DRE-1280215, R-DRE-449147
100537196	mapkap1	MAPK associated protein 1	R-DRE-168256
373081	mvp	major vault protein	R-DRE-168256, R-DRE-168249
569779	myo10	myosin X	R-DRE-168256, R-DRE-168249
557335	nlr1	NLR family member X1	R-DRE-168256, R-DRE-168249
60658	nos1	nitric oxide synthase 1 (neuronal)	R-DRE-168256, R-DRE-168249
404036	nos2a	nitric oxide synthase 2a, inducible	R-DRE-168256, R-DRE-168249
796461	nrg1	neuregulin 1	R-DRE-168256, R-DRE-1280215, R-DRE-449147
554967	psmd1	proteasome 26S subunit, non-ATPase 1	R-DRE-168256, R-DRE-168249
373104	rab14	RAB14, member RAS oncogene family	R-DRE-168256, R-DRE-168249
323197	racgap1	Rac GTPase activating protein 1	R-DRE-168256
554089	s100z	S100 calcium binding protein Z	R-DRE-168256, R-DRE-168249
402992	scamp1	secretory carrier membrane protein 1	R-DRE-168256, R-DRE-168249
793290	spred2b	sprouty related EVH1 domain containing 2b	R-DRE-168256, R-DRE-1280215, R-DRE-449147
368519	stat4	signal transducer and activator of transcription 4	R-DRE-168256, R-DRE-1280215, R-DRE-449147
492489	sugt1	SGT1 homolog, MIS12 kinetochore complex assembly cochaperone	R-DRE-168256, R-DRE-168249
405769	syk	spleen tyrosine kinase	R-DRE-168256, R-DRE-168249, R-DRE-1280215, R-DRE-449147

Gene ID	Gene	Name	Reactome Gene Sets
100333043	tap1	transporter 1, ATP-binding cassette, sub-family B (MDR/TAP)	R-DRE-168256
692289	tbk1	TANK-binding kinase 1	R-DRE-168256, R-DRE-168249, R-DRE-1280215, R-DRE-449147
100333821	tnfrsf11a	TNF receptor superfamily, member 11a, NFKB activator	R-DRE-168256, R-DRE-1280215
564279	tnip2	TNFAIP3 interacting protein 2	R-DRE-168256, R-DRE-168249, R-DRE-1280215
100331669	tpp2	tripeptidyl peptidase 2	R-DRE-168256
406335	uba1	ubiquitin-like modifier activating enzyme 1	R-DRE-168256
393934	ube2d2	ubiquitin-conjugating enzyme E2D 2 (UBC4/5 homolog, yeast)	R-DRE-168256, R-DRE-168249
406807	ube2na	ubiquitin-conjugating enzyme E2Na	R-DRE-168256, R-DRE-168249, R-DRE-1280215, R-DRE-449147
321056	zgc:63569	zgc:63569	R-DRE-168256, R-DRE-168249
393844	znrf1	zinc and ring finger 1	R-DRE-168256

Table 4 Note: R-DRE-168256: immune system, R-DRE-168249: innate immune system, R-DRE-1280215: cytokine signalling in the immune system, R-DRE-449147: signalling by interleukins

Discussion

RNA-seq compared the gene expression from uninfected control with AGD-infected gill prior to (4, 7 dpi) and after (14, 16 dpi) the appearance of AGD lesions. A total of 29.7K genes identified in naive Atlantic salmon as being altered following inoculation with *P. perurans*. No gill pathology was observed macroscopically in fish sampled up to 14 dpi, however diagnostics qPCR detected the presence of *P. perurans* on 5/6 and 6/6 fish at 4 and 7 dpi, respectively, with 17.3K genes showing altered expression during this time, demonstrating the sensitivity of this method of detection. Up-regulated immune genes were identified at 4, 14 and 16 dpi with down-regulated immune genes identified at 7 dpi.

At 4, 14 and 16 dpi, three genes CD79b, KIT proto-oncogene, receptor tyrosine kinase a (kita) and thymocyte selection associated family member 2 (themis2) were consistently up-regulated. CD79, as CD79a/CD79b heterodimers (α/β), form part of the B-cell antigen receptor (BCR) with membrane immunoglobulin molecules. The BCR complex plays a crucial role in B cell development and antibody production following antigen exposure. On activation, the B-cell receptor 'signalosome' initiates multiple signalling cascades that involves kinases, GTPases, and transcription factors resulting in changes in cell metabolism, gene expression, and cytoskeletal organisation¹⁸.

Kita is a tyrosine-protein kinase that acts as cell-surface receptor for stem cell factor (Scf) and plays an essential role in the regulation of cell survival and proliferation, hematopoiesis, stem cell maintenance, gametogenesis, mast cell development, migration and function, and in melanogenesis¹⁹.

Themis2 is a gene which encodes a protein that plays a regulatory role in both positive and negative T-cell selection during late thymocyte development. The protein functions through T-cell antigen receptor (TCR) signalling, and is necessary for proper lineage commitment and maturation of T-cells. Themis2 plays a role in the in macrophage inflammatory response, promoting LPS-induced TNF production.

Five genes were found to be up-regulated only at 14 dpi: CD99, high mobility group b3b (hmgb3b) interleukin-34 (IL-34), Lyn and tissue factor pathway inhibitor 2 (tfip2). CD99 has been described as a costimulatory molecule on T cells²⁰. High mobility group (HMG) proteins have roles in the nucleus and mitochondria as architectural DNA binding proteins, and in the cytoplasm as signalling regulators, and in the extracellular milieu as inflammatory cytokines²¹. The molecular function of HMGB3b is DNA binding and it is involved in biological processes that include regulation of transcription by RNA polymerase II and positive regulation of the innate immune response. IL-34, binding to the colony stimulating factor 1 (Csf1), increases growth or survival of monocytes. In fish as in mammals, monocytes, macrophages, and neutrophils are the main phagocytic cells²². Lyn is a Src tyrosine kinase which is also involved in the formation of a B-cell receptor 'signalosome'. Lyn also interacts with Themis2²³ and lyn activation has been reported to reduce the hypersecretion of mucus and MUC5AC in airway inflammation²⁴. Excessive mucus production in the gills is a hallmark of AGD³ with substantial up-regulation of the secreted MUC5 detected in clinical AGD¹². Specialized epithelial (goblet) cells are the major source of MUC5AC, which can be induced by MMP9 through the activation of the epidermal growth factor receptor (EGFR) and mitogen-activated protein kinase 3/2 MAPK 3/2(ERK1/2) cascade²⁵.

MAPKs are a superfamily of serine/threonine protein kinases that transduce a variety of external signals, leading to an array of cellular responses that include growth, differentiation, apoptosis, and host defence response.

The up-regulation of Lyn is only evident from 14 dpi, when mucoid patches were first identified on the gills. Tfpi2 is a serine protease inhibitor and is thought to play a role in the regulation of plasmin-mediated matrix remodelling²⁶ and in the activation of matrix metalloproteinases (MMPs) including MMP-1 and MMP-13, and to a lesser extent of MMP-2 and MMP-9²⁷.

Six genes were up-regulated only at the later times of 14 and 16 dpi, and included Bruton agammaglobulinemia tyrosine kinase (Btk), complement component 1, q subcomponent, C chain (c1qc), cyclic GMP-AMP synthase (cgas), dual adaptor of phosphotyrosine and 3-phosphoinositides (dapp1), high mobility group box 1a (hmgb1a) and IKAROS family zinc finger 1 (ikzf1) (Table 3). Btk is expressed in cells with hematopoietic lineage, with the exception of T lymphocytes and natural killer cells, and is involved in a multiple immune signalling pathways. Activated by BCR aggregation, btk constitutes a

major component of the B-cell receptor signalosome complex¹⁸ and plays a role in B-cell development and mature B-cell activation²⁸.

C1qC was up-regulated suggesting the classical complement pathway was activated. Composed of C1, C4, and C2 components reacting in this order, the classical pathway primarily recognizes antibodies in immune complexes. However, an increased expression of immunoglobulins were not observed in this study indicating that C1q is potentially interacting with other acute phase molecules.

Cgas is a cytosolic DNA sensor that activates a type-I interferon response²⁹, DAPP is a B-cell-associated adapter that regulates B-cell antigen receptor (BCR)³⁰ and ikzf1, a member of the Ikaros family of proteins are involved in lymphocyte development, including a wide range of processes, such as apoptosis, cell cycle arrest, proliferation, and differentiation³¹. Btk phosphorylates Ikaros at unique sites within the DNA binding domain, augmenting the nuclear localization and sequence-specific DNA binding activity of the transcription factor function of Ikaros³².

Analysis of the top 100 DEG lists at 7 dpi found evidence of the activation of complement and the acute phase response, with the down-regulation of chemokines, interleukins and interferon-inducible proteins and mucins.

The down-regulation of the immune response at 7 dpi identified by the reactome gene set R-DRE-168256 (Table 2) identified 51 immune-related down-regulated genes (Table 4) with 14 genes associated with R-DRE-449147: signalling by interleukins (Table 2). Further analysis of the DEGs lists at 7 dpi identified 9 interleukin (IL) genes represented by 14 individual transcripts of which 8 genes were down-regulated (IL-1 β , IL-8, IL-11, IL-12 β , IL-15, IL-17F, IL-18 and IL-34) and only one found to be up-regulated IL-27 β (Supp. Table S3).

IL-1 β has been reported as the hallmark of late stage ADG infection¹⁵ with up-regulation demonstrated in the gills with numerous lesions, fused lamellae and epithelial cells hyperplasia. The expression of IL-1 β has been associated with larger AGD-lesions, often showing greater mucous cell hyperplasia, where the mucous cells as the possible source of the IL-1 β ¹¹. Macroscopically, the progression of ADG in the current study reached gill score 1, the earliest stage in the Taylor AGD gill scoring system from 1–5. The expression of IL-1B has been associated with advance ADG lesions¹⁴ which may explain why IL-1B was not found to be up-regulated in the current study. The interleukins IL-1 β and IL-18 promote Th1 and Th17 responses³³.

The IL-17 family (IL-17A-F) signals through their correspondent receptors and activate downstream pathways that include NF- κ B, MAPKs and C/EBPs to induce the expression of antimicrobial peptides, cytokines and chemokines³⁴. IL-17, is a key cytokine produced by Th17 cells and is involved in the inflammatory and neutrophil response. A recent study¹⁰ reported the expression of IL-17A/F1b and IL-17D to be significantly down-regulated in comparison to the negative control in gills from fish inoculated with a high concentration of *P. perurans* trophozoites (5000 amoeba /L). In the current study fish were

inoculated with 2750 amoeba/L, and IL-17F was down-regulated at all 4 time points. IL-17F is mainly involved in mucosal host defence mechanisms³⁵.

IL-27 β , was the only interleukin significantly induced at 7 dpi. IL-27 is composed of two non-covalently linked subunits, IL-27p28 (p28) and IL-27 β , also called Epstein-Barr-virus-induced molecule 3 (EBI3)³⁶. These subunits exhibit structural and sequence homology to IL-12 subunits and IL-6³⁷. IL-27 is unique in that although it induces Th1 differentiation, the same cytokine suppresses immune responses. IL-27 can antagonise the development of the Th17-cell response and limit Th-17 driven inflammation³⁸ which are critical for host defence against bacterial, fungal and viral infections at mucosal surfaces³⁹.

Of the down-regulated immune genes in reactome R-DRE-168256 at 7 dpi (Table 4), 8 genes were found to participate in the Nod-like receptor signalling pathway. Nod-like receptors (NLRs) can initiate or regulate host defence pathways through formation of signalling platforms that subsequently trigger the activation of inflammatory caspases and NF- κ B⁴⁰. Genes found to participate in the Nod-like receptor signalling pathway included *cxcl8*, *hsp90AB1*, *ikkbk*, *irf9*, *mapk3*, *nlr1*, *sugt1*, and *tbk1*. Nod-like receptors (NLRs) sense pathogen-associated molecular patterns (PAMPs) (pathogens/foreign) or damage-associated molecular patterns (cells/self)⁴¹. *Irx1* is a dsRNA receptor⁴² and was identified as being down-regulated in our data set at all 4 time points (4, 7, 14 and 16 dpi).

Genes were also identified with involvement in B-cell receptor (BCR) signalling (*ikkbk*, *mapk3*, *sky*), T-cell receptor (TCR) signalling (*dlg1*, *ikkbk*, *mapk3*) and in the differentiation of Th1/Th2 (*ikkbk*, *jak3*, *mapk3*, *stat4*) and Th17 cells (*hsp90ab1*, *ikkbk*, *jak3*, *mapk3*).

Interestingly, all of these signalling pathways had 2 genes in common: *inhibitor of nuclear factor kappa B kinase subunit beta* (*ikkbk*) and mitogen-activated protein kinase 3 (*mapk3*).

The transcription factor Nuclear Factor-kappa beta (NF- κ B), prior to activation, is held in the cytoplasm by the attachment of inhibitor kappa beta (κ B) and the formation of the κ B/NF- κ B complex

ikkbk is a gene which encodes the enzyme κ B kinase beta (IKK β) which can phosphorylate 2 serine residues on the inhibitor in the κ B/NF- κ B complex, leading to the dissociation and degradation of the κ B inhibitor and the subsequent activation of NF- κ B⁴³. The dissociated NF- κ B can translocate into the nucleus and activate the transcription of hundreds of genes involved in immune response, growth control, or protection against apoptosis. IKK β is critical for cytokine production via NF- κ B activation. The initial innate immune response is under the control of IKK β and culminates in a successful humoral response that is dependent on IKK α ⁴⁴. *Mapk3* acts upstream of IKK β in the canonical NF- κ B activation pathway⁴⁵.

This is the first study exploring the transcriptomic response of Atlantic salmon to *P. perurans* in a controlled environment. The data presented show that the host response of Atlantic salmon is activated in advance of any clinical symptoms developing on gill tissue of fish inoculated with *P. perurans*. Of particular interest is the immune suppression brought about through the downregulation of 2 key genes,

ikkb and mapk3/ERK1 resulting in the continued inhibition of NF- κ B by I κ B in the cytoplasm. Pathogens have previously been reported to developed strategies to circumvent the activation of the NF- κ B activation, by preventing the inhibitor, I κ B, from being ubiquitinated and therefore preventing its degradation, causing NF- κ B to remain sequestered in the cell cytoplasm and therefore inactive⁴⁶. Indeed, some viruses encode virulence factors, for example vaccinia viral protein B14, that target IKK β to inhibit NF- κ B-mediated antiviral immune response⁴⁷, suggesting that virulence factors associated with *P. perurans* potentially have some of immunomodulatory effect on their host. The present study provides the initial discovery and description of genes showing differential expression during early-phase ADG exposure/infection, which provides the basis for future, more in-depth studies of AGD-related immune response pathways in Atlantic salmon.

Methods

Fish husbandry

Post-smolt Atlantic salmon (70g) were distributed into 4 circular black 1000 L tanks connected to recirculating aquaculture systems at a stocking density of 3.6 kg m⁻³, water temperature 12°C, artificial seawater (30PSU), and 14h/8h light/dark cycle. Fish were fed a commercial salmon diet at 1% body weight per day. The *in-vivo* fish trial was carried out according to the ARRIVE guidelines for animal research⁴⁸. This project was authorised by the Health Products Regulatory Authority (HPRA), authorisation number AE19137/P001, in compliance with Directive 2010/ 63/EU transposed into Irish law by S.I. No 543 of 2012.

Paramoeba perurans isolation and culture

P. perurans trophozoites were collected by gill swabbing from AGD infected Atlantic salmon on a commercial Irish farm. Amoebae were cultured on marine yeast agar plates (MYA; 0.01% malt, 0.01% yeast, 2% Bacto Agar), 16°C overlaid with 7 ml sterile seawater⁴⁹, and sub-cultured weekly by transferring free-floating cells to fresh MYA plates. Confirmation of *P. perurans* identity was performed using qPCR as previously described by Downes (2015)⁵.

Paramoeba perurans challenge

After an acclimatisation period of 6 days, 90 fish (45 x 2) were challenged with *P. perurans* (2750 amoebae/L) in 300 L for 4 h with oxygen saturation, fish behaviour and welfare closely monitored. Controls, 90 fish (45 x 2) were also held at 300 L for 4 h. Following holding in challenge or control tanks, fish were placed into new tanks containing 1000 L seawater.

Sample collection

Fish were euthanised by overdose of anaesthetic (400 mg L⁻¹ tricaine methane sulfonate).

Gill tissues, following perfusion with phosphate buffered saline (1x PBS), were collected from six fish at 0 dpi (pre-ADG challenge), 4, 7, 14 and 16 dpi. The 2nd left gill arch was collected from individual fish, the arch cartilage, immersed in RNA^{later}® (Ambion Inc, Austin, Texas), stored at 4°C overnight, followed by final storage at -80°C.

Disease progression

Disease progression was monitored using gill scoring carried out on euthanised fish (Taylor, 2009). Whole gill samples were taken for qPCR⁵ and histology to confirm the presence of *P. perurans*. For histological analyses, samples were fixed in 10% neutral buffered formalin, routinely processed, embedded in paraffin wax blocks, sectioned (3–5 µm), and stained with haematoxylin and eosin (H&E).

Total RNA extraction

Total RNA was extracted from 30mg gill tissue using the RNeasy® Plus Mini Kit (Qiagen) according to manufacturer's instructions. RNA was quantified using the Qubit® RNA Assay Kit in Qubit® 2.0 Fluorometer (Life Technologies, CA, USA). RNA integrity (RIN) was assessed using the RNA Nano 6000 Assay Kit of the Bioanalyzer 2100 system (Agilent Technologies, CA, USA). Total RNA with RIN ≥ 8.0 or higher were used for RNA-seq.

Library construction and transcriptome sequencing

Total RNA from 6 individual fish from at each of the 5 time points; 0, 4, 7, 14, and 16 dpi was used for the construction of 5 sequencing libraries generated using NEBNext® Ultra™ RNA Library Prep Kit for Illumina® (NEB, USA) according to manufacturer's instructions. Index codes were added to attribute sequences to each sample. The clustering of the index-coded samples was performed on a cBot Cluster Generation System using HiSeq PE Cluster Kit cBot-HS (Illumina) according to the manufacturer's instructions. After cluster generation, library preparations were sequenced on an Illumina HiSeq platform and 125 bp/150 bp paired-end reads were generated. FastQC was utilised for quality assessment of reads from each sample (Version 0.11.8) and MultiQC (Version 1.7) was used to visualise all FastQC results. Trimmomatic (v0.36) was used to trim paired reads in FASTQ files, using default parameters for paired-end mode and a minimum read length of 50bp.

Read mapping to the Atlantic salmon (*Salmo salar*) reference genome

The *Salmo salar* genome (https://www.ncbi.nlm.nih.gov/assembly/GCF_000233375.1)

was used to map the reads (supplementary Table S1 online). Mapping was implemented using HiSat2 (version 2.1.0) using default parameters and paired-end mode. Counts were generated using featureCounts (v1.6.0) using the default parameters for paired-end reads. RNA-seq specific QC, sample correlation and visualisation were implemented using Seqmonk (Version 1.45.1). Correlation matrices, PCA plots, t-SNE plots and similarity trees were generated to visualise the relationships between all samples, as well as samples by time point.

Differential expression analysis

Differential expression analysis was performed on biological replicates (n = 6) from 4, 7, 14 and 16 dpi using the DESeq2 (Version 1.24.0) where each time point was compared to time 0, pre-AGD samples (Fig. 1). DESeq R provide statistical routines for determining differential expression in digital gene expression data using a model based on the negative binomial distribution. The resulting P-values were adjusted using the Benjamin and Hochberg's approach for controlling the false discovery rate. Genes with an adjusted p-value (FDR adjusted) < 0.05 found by DESeq R were assigned as differentially expressed. Eight gene lists were generated: up- and down-regulated genes at 4, 7, 14 and 16 dpi.

Protein-Protein Interaction (PPI)

PPI was carried out using STRING (version 11.0, <https://string-db.org>) on the 8 gene lists generated from the pairwise comparisons (4, 7, 14 and 16 dpi, up- and down-regulated genes) using the default settings and *Danio rerio* selected as the species of interest. Significant pathway enrichments and functional information for genes identified in the Immune System (R-DRE-168256) was carried out using STRING against the *Homo sapiens* database.

Pathway and Process Enrichment

Gene Ontology (GO) and Kyoto Encyclopedia of Genes and Genomes (KEGG) pathway mapping was performed using Metascape (metascape.org). The zebrafish (*Danio rerio*) database was used to determine GO enrichment. Pathway and process enrichment analysis was performed using the following ontology sources: KEGG Functional Sets, KEGG Pathway, GO Biological Processes, GO Cellular Components, GO Molecular Functions, KEGG Structural Complexes and Reactome Gene Sets.

A user-supplied list of 5824 genes was used as the enrichment background. Terms with a p-value < 0.01, a minimum count of 3, and an enrichment factor > 1.5 are collected and grouped into clusters based on their membership similarities.

Validation of RNA-seq data using Real-time PCR

Real-time PCR validation of the RNA-seq data from 6 individual fish at each time point was performed using 48.48 Dynamic Array™ Integrated Fluidic Circuit (IFC) chips on the Biomark HD system. Ten genes identified as being differentially regulated in the gill RNA-seq data were selected for qPCR validation, including cathelicidin 1 (*cath-1*), c-type lectin receptor A (*clr-a*), C-C motif chemokine 4 (*cxc4*), immunoresponsive 1 homolog/ (*irg1/acod1*), interleukin-8 (*il-8*), interleukin-17F (*il-17*), leukocyte cell-derived chemotaxin-2 (*lect2*), nitric oxide synthase 2, inducible (*nos2*), pentraxin-related protein (*ptx3*), and serum amyloid P- like (*sap*). Primers were designed using PrimerQuest (Integrated DNA Technologies, <https://eu.idtdna.com/>) (supplementary Table S2 online).

Reverse transcription was carried out using the GoScript (Promega) kit as per manufacturer's instructions. A pre-amplification step was adopted for the multiplex amplification of the target genes using a MiniAmp Plus PCR machine (Applied Biosystems), as per manufacturer's recommended protocols (PN 100–5875 C1, Fluidigm). The pre-amplified cDNA was treated with Exonuclease I to remove unincorporated primers prior to running on a Biomark HD, as per manufacturer's recommended protocols (PN 100–9791 B1,

Fluidigm). PCR amplification efficiency (E) was calculated for each gene of interest and the housekeeping gene by the generation of standard curves using 10-fold serial dilutions of the cDNA template (standard curve: $R^2 > 0.980$, amplification efficiency range 90–105%). Melt curve analysis was used to confirm the amplification of single, PCR products.

Statistical analysis

For pathway and process enrichment analyses, p-values < 0.01 were calculated based on the accumulative hypergeometric distribution, and q-values calculated using the Benjamin-Hochberg correction for multiple testing using Metascape (metascape.org). Kappa scores were used as the similarity metric when performing hierarchical clustering on the enriched terms, and sub-trees with a similarity of > 0.3 were considered a cluster. The most statistically significant term within a cluster was chosen to represent the cluster. For qPCR analysis, the fold change of each gene at each time point was analysed relative to the T0 control using an un-paired t-test with differences considered significant at $p < 0.05$. Ggplot2_3.2.1 in R studio Version 3.5.1 was used to generate the Spearman correlation data. Plotly.py version 4.0.0 in Python 3.7.3 was used to graph the RNA-seq and qPCR data validation data.

Declarations

Data Availability Statement

All data supporting this study are included in the results section, the supplementary material section or openly available in public databases.

Acknowledgement

We would like to thank Ankit Dwivedi for generating the RNA validation and correlation graphs. This material is based upon research supported by the Department of Agriculture, Food and the Marine under the Grant award No. 15 S 745

Competing interests

The author(s) declare no competing interests.

Author contributions

E.M., I.O.C. L.M., J.C. conceived the project.

A.T. and L.M. contributed to the design of the experiments.

A.T., G.M., L.G., L.P., performed the experiments, contributed to the collection and analysis of data.

A.T., L.G., L.P. conducted statistical analysis.

A.T. and E.M. wrote the paper. All authors edited the paper.

References

1. Munday, B. L. Diseases of salmonids: Proceedings of the Workshop on Diseases of Australian fish and shellfish.(Department of Agriculture and Rural Affairs, 1986).
2. Oldham, T., Rodger, H. & Nowak, B. F. Incidence and distribution of amoebic gill disease (AGD) - An epidemiological review. *Aquaculture* vol. 457 35–42(2016).
3. Adams, M. B. & Nowak, B. F. Amoebic gill disease: sequential pathology in cultured Atlantic salmon, *Salmo salar* L. *J. Fish Dis.***26**, (2003).
4. Taylor, R. S., Muller, W. J., Cook, M. T., Kube, P. D. & Elliott, N. G. Gill observations in Atlantic salmon (*Salmo salar*, L.) during repeated amoebic gill disease (AGD) field exposure and survival challenge. *Aquaculture*. **290**, 1–8 (2009).
5. Downes, J. *et al.* A longitudinal study of amoebic gill disease on a marine Atlantic salmon farm utilising a real-time PCR assay for the detection of *Neoparamoeba perurans*. *Aquac. Environ. Interact.* **7**, 239–251 (2015).
6. Hamish, D. & Rodger Amoebic gill disease (AGD) in farmed salmon (*Salmo salar*) in Europe. *Fish Vet. J.* **14**, 16–27 (2014).
7. Morrison, R. N. *et al.* Transcriptome profiling the gills of amoebic gill disease (AGD)-affected Atlantic salmon (*Salmo salar* L.): a role for tumor suppressor p53 in AGD pathogenesis? *Physiol. Genomics***26**, (2006).
8. Wynne, J. W. *et al.* Transcriptome analyses of amoebic gill disease-affected atlantic salmon (*Salmo salar*) tissues reveal localized host gene suppression. *Mar. Biotechnol.* **10**, 388–403 (2008).
9. Young, N. D., Cooper, G. A., Nowak, B. F., Koop, B. F. & Morrison, R. N. Coordinated down-regulation of the antigen processing machinery in the gills of amoebic gill disease-affected Atlantic salmon (*Salmo salar* L.). *Mol. Immunol.* **45**, 2581–2597 (2008).
10. Benedicenti, O., Collins, C., Wang, T., McCarthy, U. & Secombes, C. J. Which Th pathway is involved during late stage amoebic gill disease? *Fish Shellfish Immunol.* **46**, 417–425 (2015).
11. Bridle, A. R., Morrison, R. N., Cunningham, C., Nowak, B. F. & P. M. & Quantitation of immune response gene expression and cellular localisation of interleukin-1 β mRNA in Atlantic salmon, *Salmo salar* L., affected by amoebic gill disease (AGD). *Vet. Immunol. Immunopathol.* **114**, 121–134 (2006).
12. Marcos-López, M. *et al.* Gene expression analysis of Atlantic salmon gills reveals mucin 5 and interleukin 4/13 as key molecules during amoebic gill disease. *Sci. Rep.***8**, (2018).
13. Morrison, R. N. *et al.* Molecular cloning and expression analysis of tumour necrosis factor- α in amoebic gill disease (AGD)-affected Atlantic salmon (*Salmo salar* L.). *Fish Shellfish Immunol.* **23**, 1015–1031 (2007).
14. Pennacchi, Y., Leef, M. J., Crosbie, P. B. B., Nowak, B. F. & Bridle, A. R. Evidence of immune and inflammatory processes in the gills of AGD-affected Atlantic salmon, *Salmo salar* L. *Fish Shellfish Immunol.* **36**, 563–570 (2014).

15. Pennacchi, Y., Adams, M. B., Nowak, B. F. & Bridle, A. R. Immune gene expression in the gills of Atlantic salmon (*Salmo salar* L.) following experimental reinfection with *Neoparamoeba perurans*. *Aquaculture*. **464**, 410–419 (2016).
16. Boison, S. A., Gjerde, B., Hillestad, B., Makvandi-Nejad, S. & Moghadam, H. K. Genomic and transcriptomic analysis of amoebic gill disease resistance in Atlantic salmon (*Salmo salar* L.). *Front. Genet.* **10**, (2019).
17. Marcos-López, M. *et al.* Oxidative stress is associated with late-stage amoebic gill disease in farmed Atlantic salmon (*Salmo salar* L.). *J. Fish Dis.* **41**, 383–387 (2018).
18. Takata, M. & Kurosaki, T. *A Role for Bruton's Tyrosine Kinase in B Cell Antigen Receptor-mediated Activation of Phospholipase C- β* . vol.184(1996).
19. Roskoski, R. Structure and regulation of Kit protein-tyrosine kinase - The stem cell factor receptor. *Biochemical and Biophysical Research Communications*. **338**, 1307–1315 (2005).
20. Wingett, D., Forcier, K. & Nielson, C. P. A Role for CD99 in T Cell Activation. *Cell. Immunol.* **193**, (1999).
21. Goodwin, G. H., Sanders, C. & Johns, E. W. A New Group of Chromatin-Associated Proteins with a High Content of Acidic and Basic Amino Acids. *Eur. J. Biochem.* **38**, 14–19 (1973).
22. Esteban, M. A., Cuesta, A., Chaves-Pozo, E. & Meseguer, J. Phagocytosis in teleosts. Implications of the new cells involved. *Biology (Basel)*. **4**, 907–922 (2015).
23. Peirce, M. J. *et al.* Themis2/ICB1 is a signaling scaffold that selectively regulates macrophage toll-like receptor signaling and cytokine production. *PLoS One* **5**, (2010).
24. Wang, X. *et al.* Lyn regulates mucus secretion and MUC5AC via the STAT6 signaling pathway during allergic airway inflammation. *Sci. Rep.* **7**, 1–13 (2017).
25. Deshmukh, H. S. *et al.* Metalloproteinases mediate mucin 5AC expression by epidermal growth factor receptor activation. *Am. J. Respir. Crit. Care Med.* **171**, 305–314 (2005).
26. Chand, H. S., Foster, D. C. & Kisiel, W. Structure, function and biology of tissue factor pathway inhibitor-2. *Thromb. Haemost.* **94**, 1122–1130 (2005).
27. Herman, M. P. *et al.* Tissue factor pathway inhibitor-2 is a novel inhibitor of matrix metalloproteinases with implications for atherosclerosis. *J. Clin. Invest.* **107**, 1117–1126 (2001).
28. Jefferies, C. A. *et al.* Bruton's tyrosine kinase is a Toll/interleukin-1 receptor domain-binding protein that participates in nuclear factor κ B activation by toll-like receptor 4. *J. Biol. Chem.* **278**, 26258–26264 (2003).
29. Wu, J. *et al.* Cyclic GMP-AMP is an endogenous second messenger in innate immune signaling by cytosolic DNA. *Science (80-)*. **339**, 826–830 (2013).
30. Marshall, A. J. *et al.* A Novel B Lymphocyte-associated Adaptor Protein, *Bam32*, Regulates Antigen Receptor Signaling Downstream of Phosphatidylinositol 3-Kinase. *J. Exp. Med.* vol. 191 <http://www.jem.org/cgi/current/full/191/8/1319> (2000).
31. Fan, Y. & Lu, D. The Ikaros family of zinc-finger proteins. *Acta Pharm. Sin. B* **6**, (2016).
32. Ma, H. *et al.* Regulatory Phosphorylation of Ikaros by Bruton's Tyrosine Kinase. *PLoS One* **8**, (2013).

33. Sims, J. E. & Smith, D. E. The IL-1 family: Regulators of immunity. *Nature Reviews Immunology*. **10**, 89–102 (2010).
34. Chang, S. H. & Dong, C. Signaling of interleukin-17 family cytokines in immunity and inflammation. *Cell. Signal.* **23**, 1069–1075 (2011).
35. Lee, Y., Clinton, J., Yao, C. & Chang, S. H. Interleukin-17D promotes pathogenicity during infection by suppressing CD8 T Cell activity. *Front. Immunol.* **10**, (2019).
36. Pflanz, S. *et al.* IL-27, a heterodimeric cytokine composed of EBI3 and p28 protein, induces proliferation of naive CD4 + T cells. *Immunity*. **16**, 779–790 (2002).
37. Rousseau, F. *et al.* IL-27 structural analysis demonstrates similarities with ciliary neurotrophic factor (CNTF) and leads to the identification of antagonistic variants. *Proc. Natl. Acad. Sci. U. S. A.* **107**, 19420–19425(2010).
38. Goriely, S., Neurath, M. F. & Goldman, M. *How microorganisms tip the balance between interleukin-12 family members.* (2008).
39. Yoshida, H., Nakaya, M. & Miyazaki, Y. Interleukin 27: a double-edged sword for offense and defense. *J. Leukoc. Biol.* **86**, 1295–1303 (2009).
40. Gurung, P. & Kanneganti, T. D. Immune responses against protozoan parasites: a focus on the emerging role of Nod-like receptors. *Cellular and Molecular Life Sciences*. **73**, 3035–3051 (2016).
41. Proell, M., Riedl, S. J., Fritz, J. H., Rojas, A. M. & Schwarzenbacher, R. The Nod-Like Receptor (NLR) family: A tale of similarities and differences. *PLoS One* **3**, (2008).
42. Nagai-Singer, M. A., Morrison, H. A. & Allen, I. C. NLRX1 Is a Multifaceted and Enigmatic Regulator of Immune System Function. *Frontiers in Immunology* vol. 10 (2019).
43. Tsuchiya, Y. *et al.* Nuclear IKK β Is an Adaptor Protein for I κ B α Ubiquitination and Degradation in UV-Induced NF- κ B Activation. *Mol. Cell* **39**, (2010).
44. Bonizzi, G. & Karin, M. The two NF- κ B activation pathways and their role in innate and adaptive immunity. *Trends Immunol.* **25**, 280–288 (2004).
45. Gamble, C. *et al.* Inhibitory kappa B kinases as targets for pharmacological regulation. *British Journal of Pharmacology*. **165**, 802–819 (2012).
46. Angot, A., Vergunst, A., Genin, S. & Peeters, N. Exploitation of eukaryotic ubiquitin signaling pathways by effectors translocated by bacterial type III and type IV secretion systems. *PLoS Pathogens*. **3**, 0001–0013 (2007).
47. Tang, Q., Chakraborty, S. & Xu, G. Mechanism of vaccinia viral protein B14-mediated inhibition of I κ B kinase β activation. *J. Biol. Chem.* **293**, (2018).
48. Kilkenny, C., Browne, W., Cuthill, I. C., Emerson, M. & Altman, D. G. Animal research: Reporting in vivo experiments: The ARRIVE guidelines. *Br. J. Pharmacol.* **160**, 1577–1579 (2010).
49. Crosbie, P. B. B., Bridle, A. R., Cadoret, K. & Nowak, B. F. In vitro cultured Neoparamoeba perurans causes amoebic gill disease in Atlantic salmon and fulfils Koch's postulates. *Int. J. Parasitol.* **42**, 511–515 (2012).

Figures

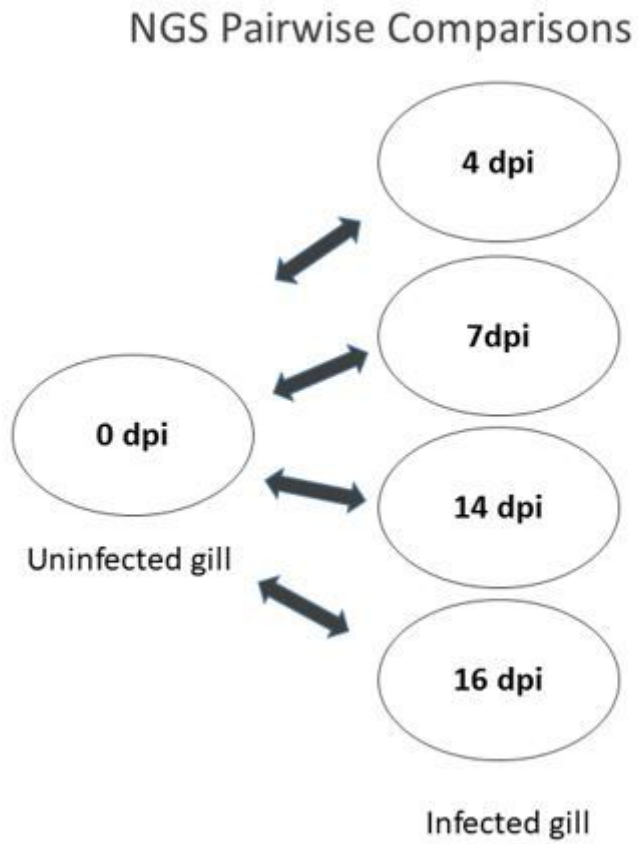


Figure 1

Experimental design of Next Generation Sequencing (NGS) pairwise comparisons. Gill samples for RNA sequencing were collected at 0, 4, 7, 14 and 16 dpi. Each post-infection time point was compared back to the pre-AGD, 0 dpi time point.

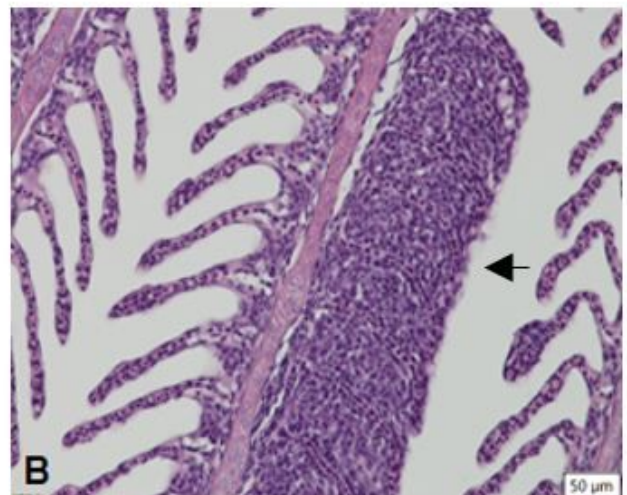
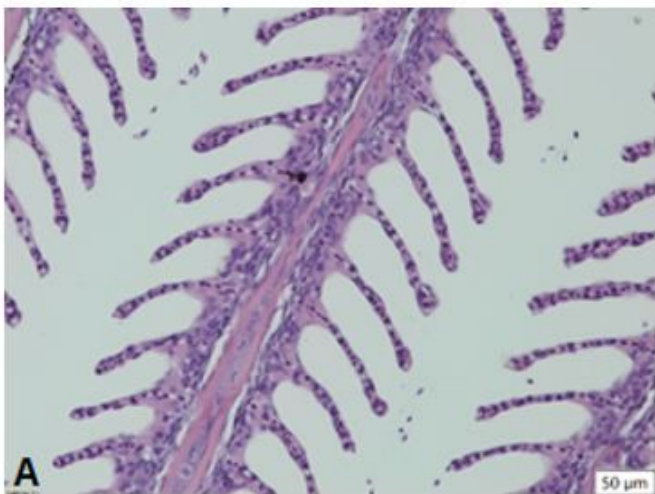


Figure 2

(a) Gill histology in AGD at 0 dpi and (b) at 16 dpi. The arrow in (b) indicates an area of lamellar fusion in the gill that occurred as a result of AGD infection. Scale is 50 μ m

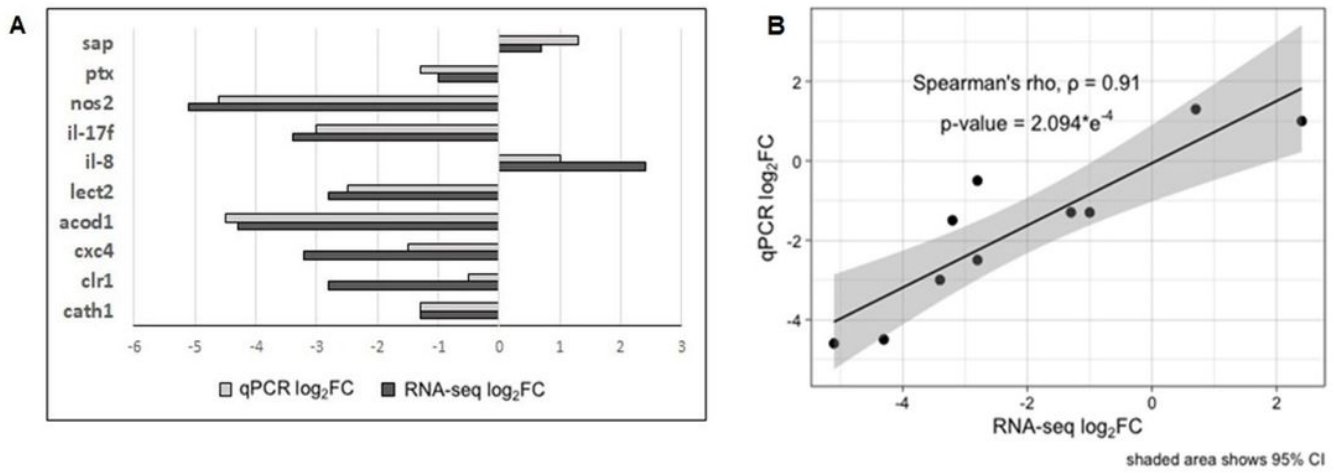
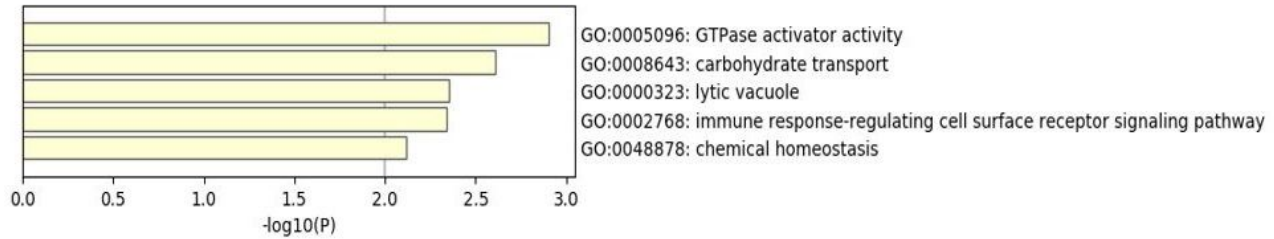
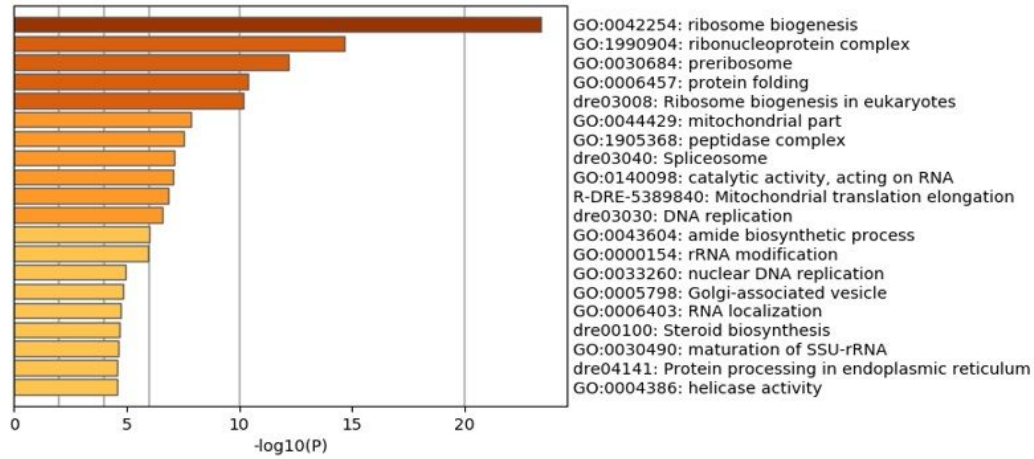


Figure 3

(A) Validation of RNA-seq data using qPCR (B) Spearman correlation analysis of RNA-seq and qPCR data.



A



B

Figure 4

(A): Enriched GO terms in the gill at 4 dpi for up-regulated DEGs. (B): Enriched GO terms in the gill at 4 dpi for down-regulated DEGs.

Supplementary Files

This is a list of supplementary files associated with this preprint. Click to download.

- [TranscriptomicResponseinAtlanticsalmonSupplementarymaterial.docx](#)